Hindawi
International Journal of Antennas and Propagation
Volume 2019, Article ID 1604695, 8 pages
https://doi.org/10.1155/2019/1604695

Research Article

Design of Modified Single-Layer Double U-Type Linear to Circular Polarization Convertor

Haoming Hu, Dongfang Zhou, Guohu Chen, Tianpeng Li, and Jun Gao

National Digital Switching System Engineering and Technological R&D Center, Zhengzhou, Henan 450000, China

Correspondence should be addressed to Haoming Hu; hhmseu2012@163.com

Received 14 November 2018; Accepted 30 December 2018; Published 3 March 2019

Academic Editor: Chien-Jen Wang

Copyright © 2019 Haoming Hu et al. This is an open access article distributed under the Creative Commons Attribution License, which permits unrestricted use, distribution, and reproduction in any medium, provided the original work is properly cited.

This paper proposes single-layer periodic arrays of freestanding slot frequency-selective surface (FSS) as an approach to convert linearly polarized wave to circularly polarized wave. The double U-type structure is etched on a metal plate rather than a traditional print circuit board (PCB) material. It has the characteristics of broadband and could be applied to the situation of large incident angles. Numerical simulations have been carried out, and the prototype structures have been fabricated and experimentally validated. The whole thickness is only 1 mm, and the results show that 3 dB axial ratio (AR) bandwidth is 36.6% at normal incident (16.5% at ±60°). An insertion loss of under 3 dB can be achieved within the whole AR bandwidth.

1. Introduction

In recent years, circularly polarized antennas using polarization transformers are widely used in fields such as satellite communications, telemetry, and electronic warfare for eliminating rain echoes or for the suppression of interference. Therefore, the research on transmission-type polarizers has become a hot issue, which, when placed over a radiating aperture, convert linearly polarized (LP) signals into circularly polarized (CP) signals [1]. Nowadays, most technologies of the transformation of linear to circular polarization are based on frequency-selective surface (FSS), which is an important component in antenna systems especially in beam-scanning antennas [2].

There are several methods designing transmission-type polarizers. One is based on polarizers made in PCB technology such as Ref. [3], wherein Fei et al. proposed a novel single-layer linear to circular polarizer which consists of hybrid meander line and loop configuration. Although it is characterized by a wide band, its insertion loss exceeds 3 dB. Typical two [4] and three layers [5], even multilayers [6], have been studied extensively. Universally, an approach focus on designing a multilayer polarizer was presented by Blanco and Sauleau in [7]. The main drawback of PCB polarizers is that their performance abruptly deteriorates for a large angle of incidence, which restricts their use for beam-scanning antennas. Ratni et al. proposed a linear to circular polarization convertor using a reconfigurable metasurface which can be tuned in frequency by changing the applied voltage along the metasurface [8]. The concept of this method is advanced. A wide-band circular polarization convertor using ultrathin bilayered metasurfaces is proposed which is composed of two layers of metallic pattern arrays separated by a 1.5 mm thick dielectric spacer [9].

Another method is slotting on metal directly. Euler et al. proposed three types of a split ring polarization convertors, cross-slot, ring slot, and hexagonal slot for single and double layers. The maximum 3 dB axial ratio bandwidth for a single layer is 21% at normal incidence and only 8% at 45 degrees [10], which is not suitable for beam-scanning antennas, neither. Based on these structures, sub-mm wet etched linear to circular polarization converters are proposed in [11]. Zelenchuk and Fusco have given the first report of a planar phase plate structure based on frequency-selective surface (FSS) technology for the generation of helical far-field radiation patterns with circular polarization properties which demonstrated that the structure of a split ring could obtain progressive rotational phase shift [12]. Although the

technology of a linear to circular polarization convertor is quite mature, the performance of broadband and large angle of incidence still could be optimized [13].

In this paper, a modified double U-type split ring linear to circular polarization convertor is proposed. It has a better performance on bandwidth and oblique incident that will be introduced in the following sections. This paper is organized in the following manner: Section 2 discusses the configuration and design principle of the proposed linear to circular polarizer. In Sections 3 and 4, the simulated and measured results of the designed polarizer are presented and analyzed. Finally, a brief conclusion is given in Section 5.

2. Design and Operating Principle

In this section, the topology of the proposed structure and operating principle will be analyzed. Figure 1 shows the schematic model of a linear to circular polarization convertor.

Assume that a linearly polarized wave was titled 45 degrees relative to the x- and y-axis, normally incident onto the single-layer periodic structure. The incident wave can be decomposed to obtain two orthogonal wave components that have the same amplitude and phase, one in the vertical direction and the other in the horizontal direction. When passing through the polarization convertor, the amplitude of the transmitted coefficient for each component is ideally equal, but two distinct phase shifts on the two components should be taken into consideration [14]. If the conditions of equal amplitude and 90° differential phase between the two components are met, the transmitted wave will be perfectly circularly polarized. These two necessary conditions could be expressed by

$$\beta = \frac{\left|E_x^t\right|}{\left|E_y^t\right|} = 1,$$
$$\Delta\varphi = \varphi_x^t - \varphi_y^t = \frac{n\pi}{2}, \quad n = \pm 1, \pm 3, \pm 5, \ldots, n, \tag{1}$$

where $|E_x^t|$ and $|E_y^t|$ are the amplitudes of transmitted wave and φ_x^t and φ_y^t are the phases of transmitted wave in the x and y direction components, respectively.

Therefore, the key point to design a linear to circular polarization convertor is how to meet the amplitude and phase conditions. When rotated with respect to an incident linearly polarized signal, a circular or rectangle split ring will produce a variation of both the amplitude and phase in the signal reflected from it or through it [15]. Based on this principle, we propose a double U-type split ring CP polarization convertor. The unit cell of the structure is shown in Figure 2.

The structure consists of two U-type slots on the metal plate heading different directions. The thickness of the metal plate is 1 mm aluminum, the manufacturing cost is much more inexpensive than the polarizers based on PCB technology, and the manufacturing difficulty is greatly reduced.

The values of parameters of the structure need to be modified to satisfy the two necessary conditions to generate a CP wave. The equal amplitude criteria can be met by using

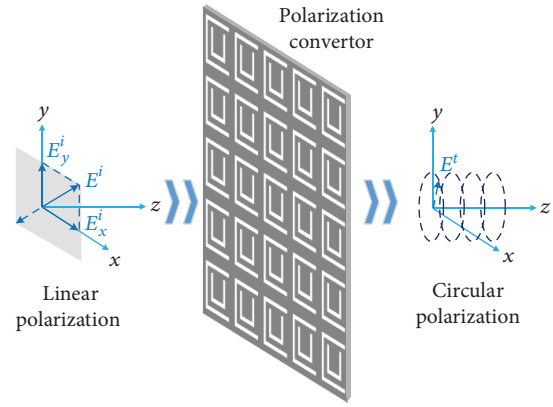

Figure 1: The schematic model of the linear to circular polarization convertor.

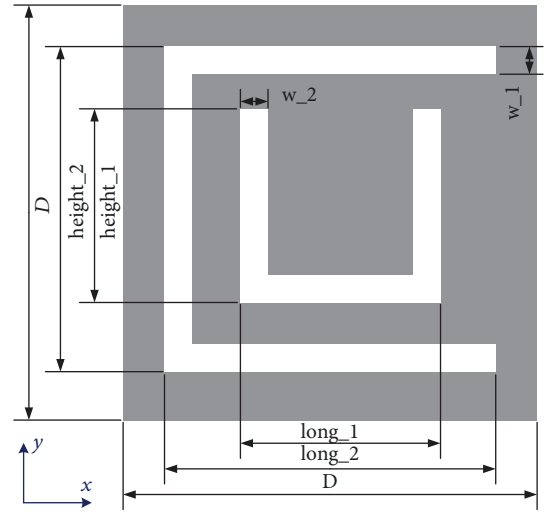

Figure 2: The unit cell of the proposed polarization convertor.

two split ring slots in a metal plate. Specifically, the amplitudes of both components could be controlled by adjusting the width of the inner and outer slots [16]. In regard to phase control, it is mainly determined by the equivalent electrical length of the inner and outer slots. With reference to the double U-type slots, the incident TE (defined in the y direction in CST) wave component causes the shorter inner slot to resonate slightly above the operating frequency of the polarizer, whereas the TM (defined in the x direction in CST) wave component causes the outer slot to resonate at a frequency slightly below. In other words, the equivalent electrical length of the inner slot is shorter leading to the phase of TE wave component which is ahead of TM's, just as shown in Figure 3 which shows the surface current distribution along one unit cell under TM and TE waves at 8.5GHz. From the picture, we can see that the surface currents of Ex and Ey reach the maximum value in the phase of 140 degrees (a) and 230 degrees (b), respectively, which indicates that the phase of transmitted wave in the x and y directions has been changed.

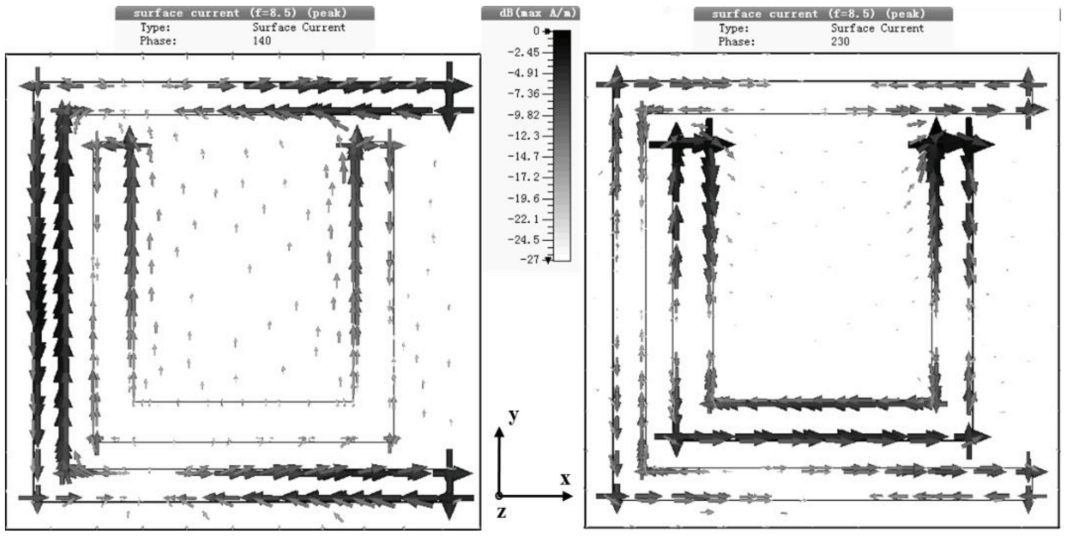

Figure 3: The surface current distribution of (a) Ex (phase = 140 deg) and (b) Ey (phase = 230 deg) at 8.5 GHz.

Table 1: Optimal parameters of the FSS.

Parameters	D	height_1	height_2	long_1	long_2	w_1	w_2
Value (mm)	17.5	11.2	13.1	8.1	15.5	1.2	1.5

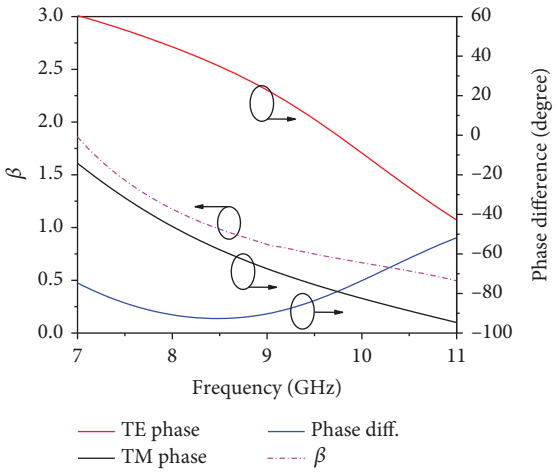

Figure 4: Simulated amplitude and phase relation with respect to frequency under normal incidence.

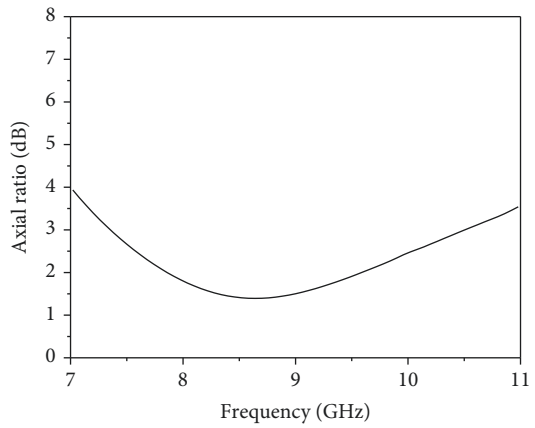

Figure 5: The simulated axial ratio of proposed FSS under normal incidence.

Therefore, the dimensions of the inner and outer slots, both the width and length, control the amplitude and phase of the transmitted wave.

3. Simulations and Sensitivity to Dimensional Variation

The simulation was carried out by using the full-wave EM solver (CST Microwave Studio). The frequency domain solver and adaptive mesh refinement were employed to perform the simulations. To reduce the computational volume to that of a single unit cell, we implemented periodic boundary conditions. The unit cell boundaries in the z direction are open which indicates that they are realized by Floquet modes [4]. After completing the preprocessing settings, we simulated the case of normal and oblique incidences, respectively.

3.1. Results at Normal Incidence. We firstly simulated at normal incidence, and a group of parameters is optimized based on the above analysis as shown in Table 1.

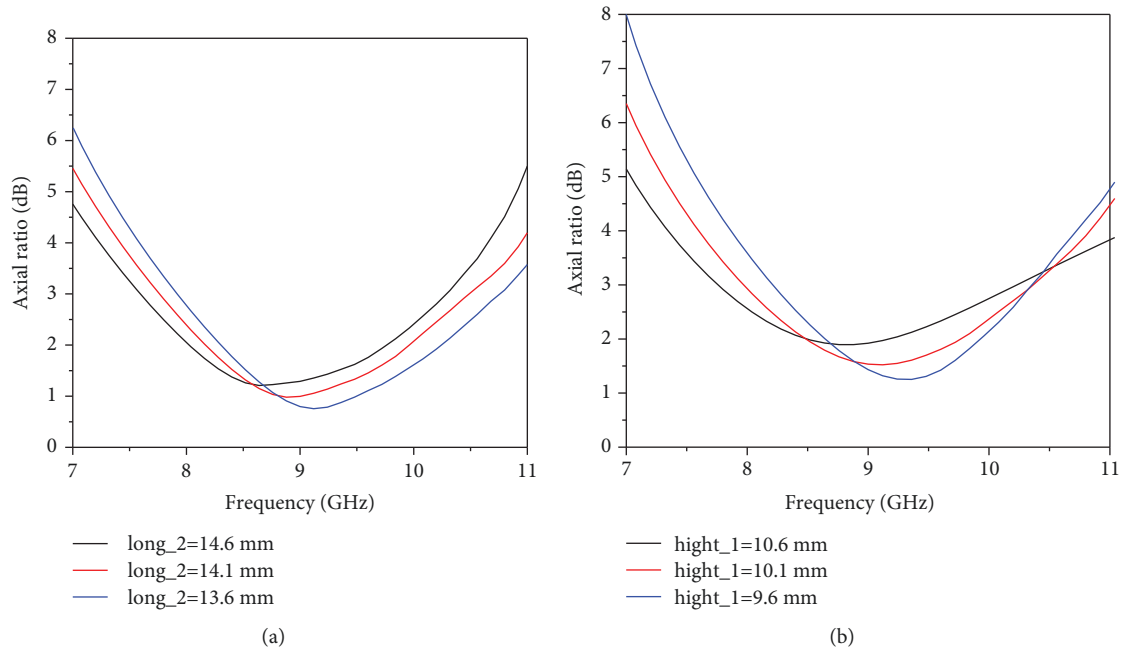

FIGURE 6: Simulated axial ratio of the proposed FSS for some main parameters: (a) the length of the outer slot and (b) the length of the inner slot.

Figure 4 shows the simulated phase difference between $\overrightarrow{E}^t_x$ and $\overrightarrow{E}^t_y$ and the amplitude relationship (β) between $|E^t_x|$ and $|E^t_y|$. The results indicate that the phase difference condition is satisfied (90 ± 10 degrees between 7.2 and 9.7GHz, 29.6% for relative bandwidth). With regard to amplitude, the bandwidth matching the condition $\beta = 1 \pm 0.25$ is from 7.6 to 9.8 GHz.

After getting the results of amplitude and phase difference, the axial ratio could be calculated in terms of β and $\Delta\varphi$ as [17]

$$\mathrm{AR} = \left[\frac{1 + \beta^2 + \sqrt{\left(1 - \beta^2\right) + 4\beta^2 \cos^2(\Delta\varphi)}}{1 + \beta^2 - \sqrt{\left(1 - \beta^2\right) + 4\beta^2 \cos^2(\Delta\varphi)}}\right]^{1/2}. \quad (2)$$

Then, the result of AR of transmitted circularly, polarized output wave, in case of 45° normally incident, linearly polarized wave, is shown in Figure 5. For an AR of less than 3 dB, the bandwidth is from 7.3 to 10.44 GHz, 35.4% for relative bandwidth; although the AR is not the optimum performance at normal incidence, it shows good performance at a large incident angle which will be analyzed in the following section.

3.2. Sensitivity to Dimensional Variation. A sensitivity analysis on the variation of parameters will be conducted in this section. All of the following simulations in this part are carried under the situation of normal incidence. Figure 6(a) demonstrates the variation of AR versus frequency with different values of the length of the outer slot, long_2. As analyzed in Section 2, reducing the length of the outer slot will reduce the equivalent electrical length of TM and has few effects on TE component, which leads to a higher resonant frequency of TM, and the phase relationship between TM and TE will be changed at the same time. Therefore, the bandwidth of AR moves to higher frequency.

Figure 6(b) shows the simulated axial ratio variation with high_1. The length of the inner slot mainly affects the TE component. When reducing high_1, the transmission coefficient of the TE component deteriorates due to the change of relative size which breaks the amplitude condition. Consequently, the 3 dB AR bandwidth becomes narrow. On the other hand, the equivalent electrical length of TE decreases, which leads to a higher resonant frequency of TE, the same trend of frequency shift as TM.

In a word, this structure is much more adjustable. The operating bandwidth could be designed by changing the length of the inner or outer slots which is easy to manufacture and cut cost.

3.3. Influence of Different Oblique Incidences. Figures 7(a) and 7(b) show the simulated AR response under oblique incidences of linearly polarized wave in the x-z and y-z planes. In the x-z plane, observe that the structure demonstrates a relatively stable operation in terms of AR of the transmitted wave over a wideband of interest for incident angles in the range of ±60°, 35.5% for 0 degree and 17.3% for ±60 degrees, respectively. With the increasing of incident angles, the deterioration of the 3 dB AR bandwidth is a normal trend which could be explained that in the case of oblique incidence, high-order mode is inspired in advance which breaks the amplitude and phase conditions. In the y-z plane, when changing incident angles, the AR response in a part of high frequency has a

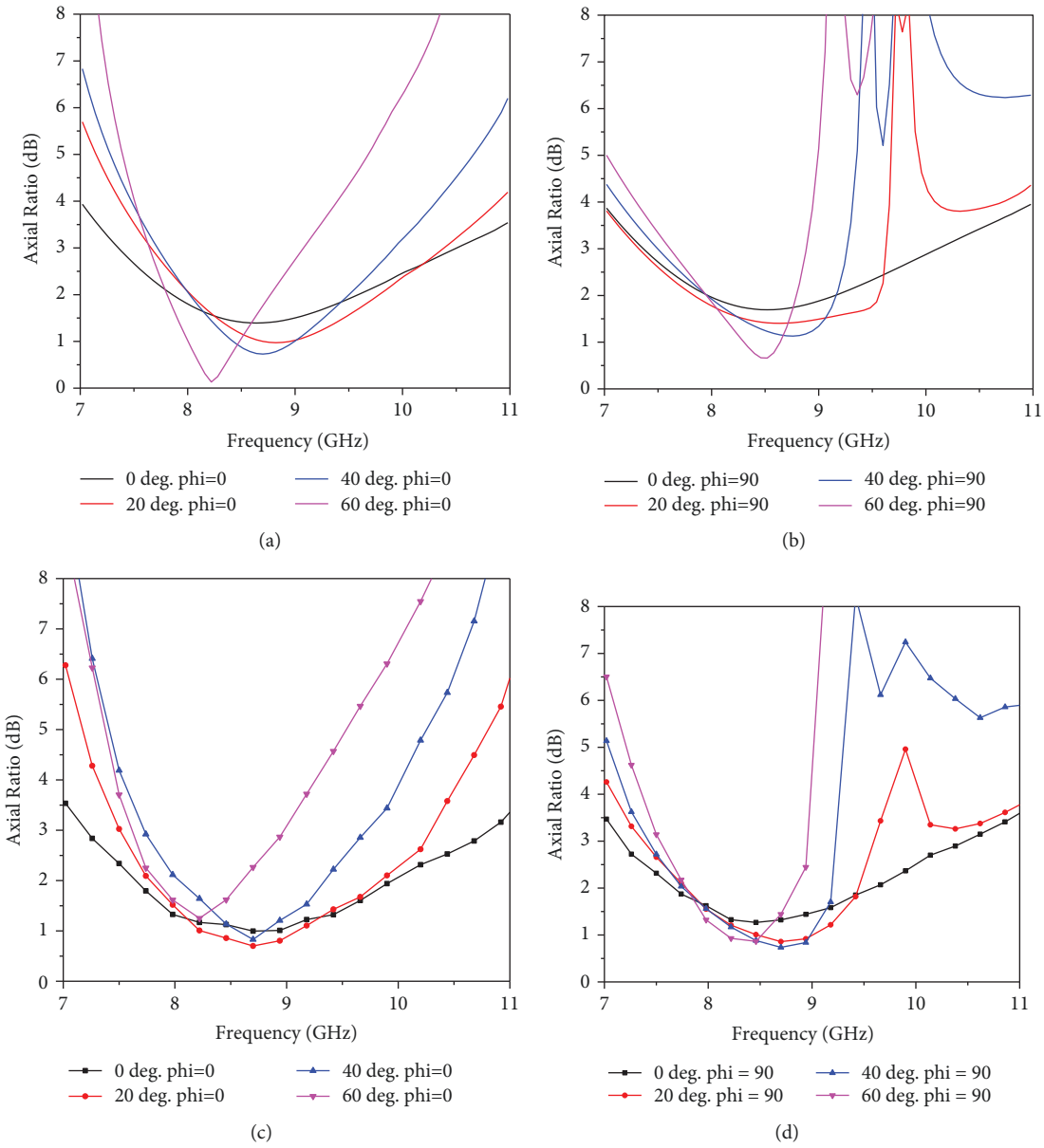

Figure 7: (a, b) Simulated and (c, d) experimental axial ratio results of the transmitted wave passed through the polarization convertor for oblique incidences of 0, 20, 40, and 60 degrees in (a, c) x-z plane and (b, d) y-z plane.

mutation which is caused by the asymmetry of the structure [18] but almost do not affect the 3 dB AR bandwidth except at the 20° incident angle.

The simulated and measured transmission and reflection coefficient results are shown in Figure 8. Considering the characteristics of FSS, with the change of oblique incidence and different incident planes, the structure has different frequency responses which causes the frequency shift. On the other hand, the manufacturing and measurement errors may cause further deterioration. In general, it can be concluded from the measured results that during the whole 3 dB AR bandwidth, the transmission coefficient is less than 3 dB which shows a good performance in application.

4. Measurements and Discussion

In order to validate the performance of the design method presented above, a single-layer double U-type polarization convertor is fabricated, as shown in Figure 9. The sensitivity of the response of the fabricated prototype to the angle of incidence was measured for various angles of incidence in the range of 0°-60° in both the x-z and y-z planes.

The measurement equipment consists of a two-port vector network analyzer (VNA) which is connected to the transmitting and receiving LP horn antennas (X band). The transmitting LP horn antenna was fed from a port of VNA and positioned at the 45° tilt angle relative to the polarization convertor. The receiving horn antenna rotates

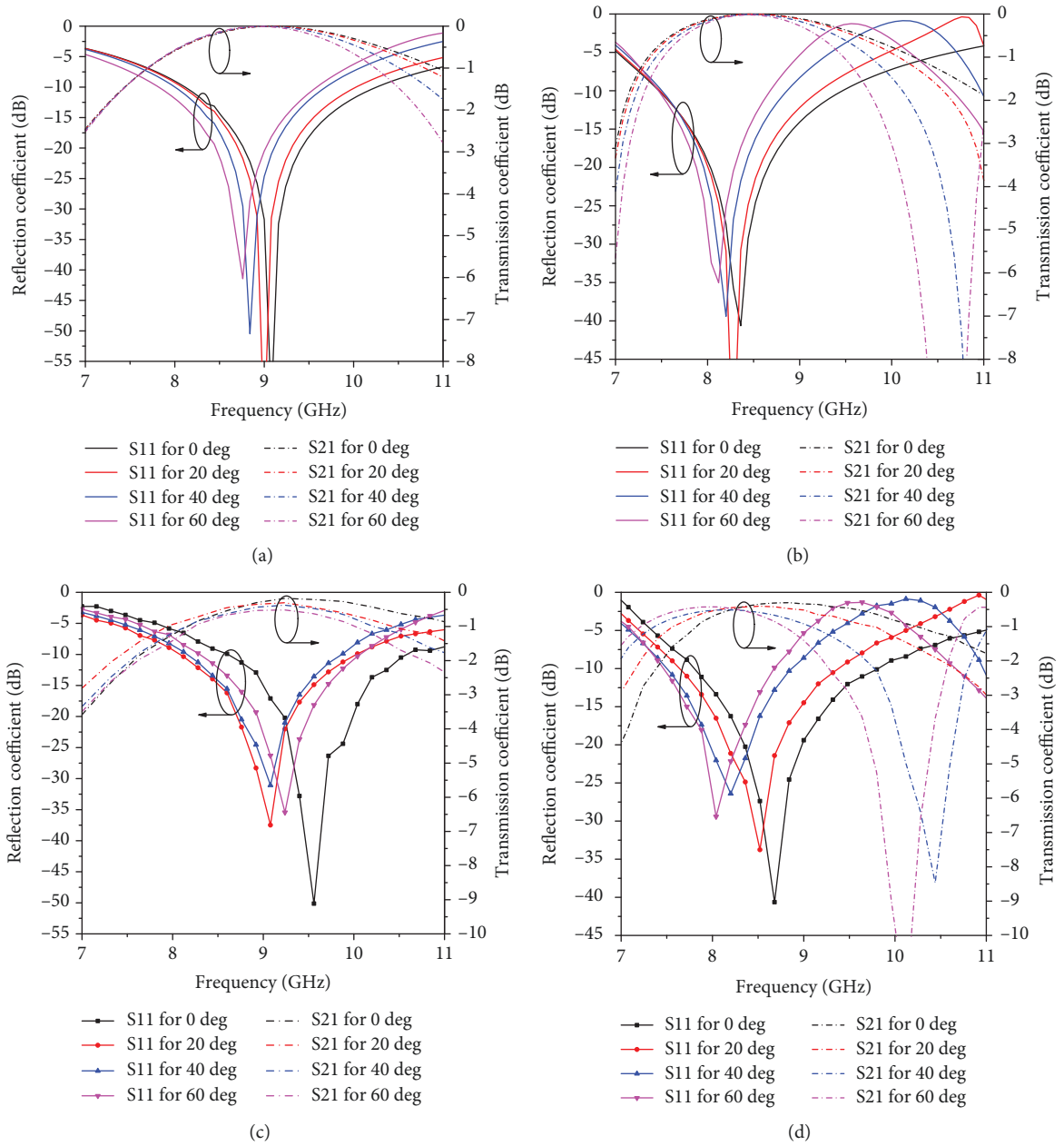

Figure 8: (a, b) Simulated and (c, d) experimental transmission and reflection coefficient results of the transmitted wave passed through the polarization convertor for oblique incidences of 0, 20, 40, and 60 degrees in (a, c) x-z plane and (b, d) y-z plane.

axially to collect the data for S21 (including magnitude and phase) at various angles. The measured data was then postprocessed to calculate the AR of the exit CP wave using Equation (2), and the results are shown in Figures 7(c) and 7(d).

There is a good consistency between the experimental and simulated results especially at small incident angles. The measured 3 dB axial ratio bandwidths of the design in the x-z plane are found to be 36.6% and 16.5% for 0 and ±60 degrees, respectively, better in 0° and slightly worse in maximum angles. About the results in the y-z plane, the measured 3 dB results show a similar trend as simulated, despite the instability in the axial ratio and the shift in frequency. These deviations may be caused by the manufacturing errors and the experimental environment.

Table 2 shows the comparison between our design and some other single-layer published polarizers. Compared with these typical structures, our design has the advantages not only in the bandwidth of normally incident but also under maximum incidence which demonstrates that our design is more suitable for beam-scanning antennas.

5. Conclusions

A modified single-layer double U-type split ring linear to circular polarization convertor is proposed in this paper.

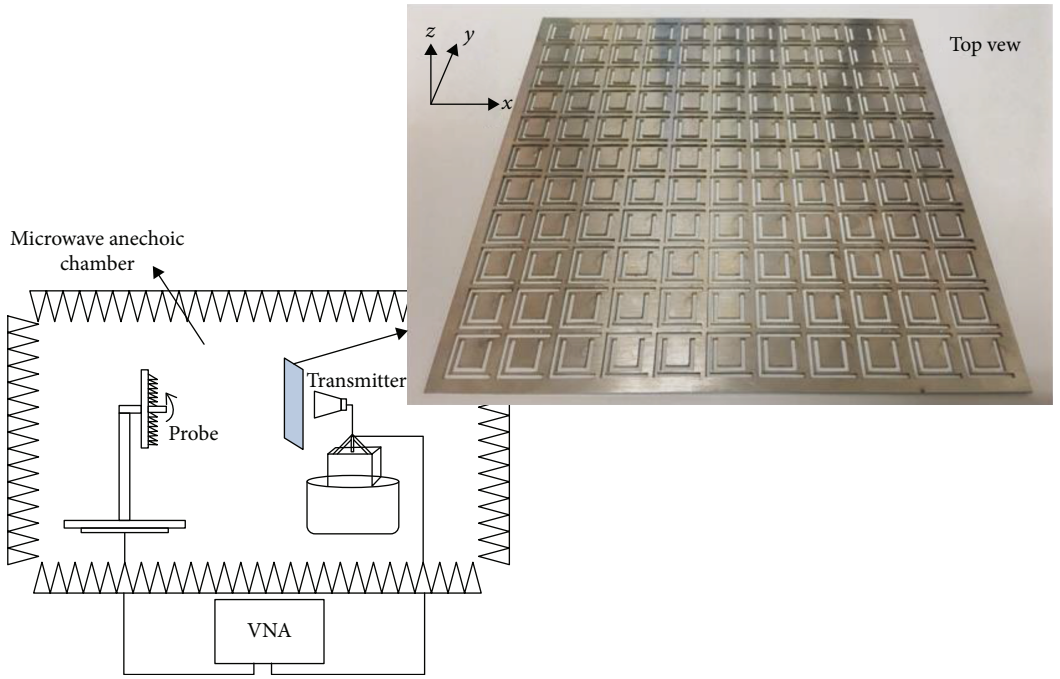

Figure 9: Photograph of the fabricated polarization and measurement environment.

Table 2: Comparisons between the proposed structure and some other single layers reported linear to circular polarizers.

Design	3 dB AR bandwidth	
	Under normal incidence	Under maximum incidence
Cross-slot structure [10]	14%	7% at ±45°
Ring slot [10]	13.3%	8.5% at ±45°
Hexagon slot [10]	10.4%	7.8% at ±45°
Ring slot [11]	21%	N/A
Annular ring with diagonal strip [19]	17%	9.8% at ±30°
Our design	36.6%	16.5% at ±60°

The double U-type structure is etched on a metal plate that reduces the process difficulty and costs significantly, and the whole thickness is only 1 mm. Numerical simulations have been carried out, and the prototype structures have been fabricated and experimentally validated. Both simulated and measured results show good performance on bandwidth and large incident angles, 36.6% for 0 deg and 16.5% for ±60 deg, which is desirable in beam-scanning antenna systems.

Data Availability

The data used to support the findings of this study are available from the corresponding author upon request.

Conflicts of Interest

The authors declare no conflict of interest.

Acknowledgments

This research was supported by the National Digital Switching System Engineering and Technological R&D Center.

References

[1] R. C. Johnson, *Antenna Engineering Handbook*, vol. 1, McGraw-Hill Education Europe, London, U.K, 3nd ed edition, 2007.

[2] J. Gao, X. Lei, G.-H. Chen, Y. Zhang, and J.-M. Wu, "Design of the variable inclination continuous transverse stub antenna based on rectangular grating slow-wave structure," *International Journal of Antennas and Propagation*, vol. 2018, Article ID 5793535, 7 pages, 2018.

[3] P. Fei, Z. Shen, X. Wen, and F. Nian, "A single-layer circular polarizer based on hybrid meander line and loop configuration," *IEEE Transactions on Antennas and Propagation*, vol. 63, no. 10, pp. 4609–4614, 2015.

[4] F. A. Mangi, S. Xiao, G. A. Mallah, D. A. Jamro, I. Memon, and G. F. Kakepoto, "Multiband circular polarizer based on fission transmission of linearly polarized wave for *X*-band applications," *Journal of Electrical and Computer Engineering*, vol. 2016, Article ID 4293089, 8 pages, 2016.

[5] M.-A. Joyal and J.-J. Laurin, "Analysis and design of thin circular polarizers based on meander lines," *IEEE Transactions on Antennas and Propagation*, vol. 60, no. 6, pp. 3007–3011, 2012.

[6] S. M. A. Momeni Hasan Abadi and N. Behdad, "Wideband linear-to-circular polarization converters based on miniaturized-element frequency selective surfaces," *IEEE Transactions on Antennas and Propagation*, vol. 64, no. 2, pp. 525–534, 2016.

[7] D. Blanco and R. Sauleau, "Broadband and broad-angle multilayer polarizer based on hybrid optimization algorithm for

low-cost Ka-band applications," *IEEE Transactions on Antennas and Propagation*, vol. 66, no. 4, pp. 1874–1881, 2018.

[8] B. Ratni, A. de Lustrac, G.-P. Piau, and S. N. Burokur, "Electronic control of linear-to-circular polarization conversion using a reconfigurable metasurface," *Applied Physics Letters*, vol. 111, no. 21, article 214101, 2017.

[9] Y. Li, J. Zhang, S. Qu et al., "Achieving wide-band linear-to-circular polarization conversion using ultra-thin bi-layered metasurfaces," *Journal of Applied Physics*, vol. 117, no. 4, article 044501, 2015.

[10] M. Euler, V. Fusco, R. Cahill, and R. Dickie, "Comparison of frequency-selective screen-based linear to circular split-ring polarisation convertors," *IET Microwaves, Antennas & Propagation*, vol. 4, no. 11, pp. 1764–1772, 2010.

[11] M. Euler, V. Fusco, R. Dickie, R. Cahill, and J. Verheggen, "Sub-mm wet etched linear to circular polarization FSS based polarization converters," *IEEE Transactions on Antennas and Propagation*, vol. 59, no. 8, pp. 3103–3106, 2011.

[12] D. Zelenchuk and V. Fusco, "Split-ring FSS spiral phase plate," *IEEE Antennas and Wireless Propagation Letters*, vol. 12, pp. 284–287, 2013.

[13] E. Sun, D. Feng, and T. Jia, "Phase- and polarization-controlled two-photon Rabi oscillation of the biexciton state in a semiconductor quantum dot," *Advances in Condensed Matter Physics*, vol. 2014, Article ID 219381, 5 pages, 2014.

[14] J.-m. Wu, D.-f. Zhou, X. Lei, J. Gao, and H.-m. Hu, "Design of a compact broadband 90° waveguide twist based on double-corner-cut square slots," *International Journal of Antennas and Propagation*, vol. 2017, Article ID 8657620, 5 pages, 2017.

[15] P. Zhou, Z. Zhang, M. He, Y. Hao, and C. Zhang, "Design of a small-size broadband circularly polarized microstrip antenna array," *International Journal of Antennas and Propagation*, vol. 2018, Article ID 5691561, 10 pages, 2018.

[16] S. H. Zainud-Deen, N. A. el-Shalaby, S. M. Gaber, and H. A. Malhat, "Circularly polarized transparent microstrip patch reflectarray integrated with solar cell for satellite applications," *International Journal of Microwave Science and Technology*, vol. 2016, Article ID 6102530, 7 pages, 2016.

[17] Y.-z. Liu, "Analysis and optimum design of wideband meander-line polarizer," *Telecommunication Engineering*, vol. 8, pp. 1334–1339, 2012.

[18] W. Zhang, J.-y. Li, and J. Xie, "A broadband linear-to-circular transmission polarizer based on right-angled frequency selective surfaces," *International Journal of Antennas and Propagation*, vol. 2017, Article ID 8067574, 6 pages, 2017.

[19] X. Ma, C. Huang, M. Pu, C. Hu, Q. Feng, and X. Luo, "Single--layer circular polarizer using metamaterial and its application in antenna," *Microwave and Optical Technology Letters*, vol. 54, no. 7, pp. 1770–1774, 2012.

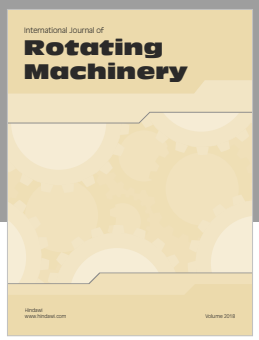

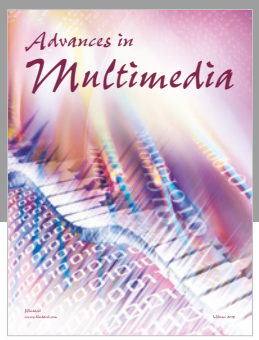

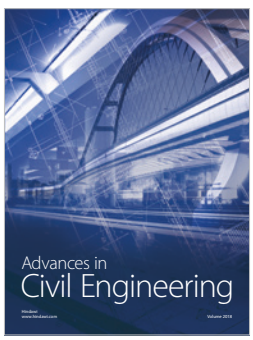

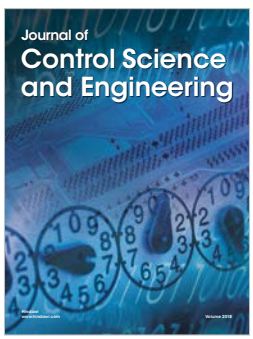

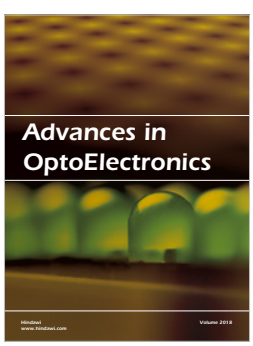

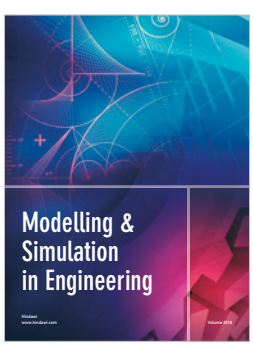

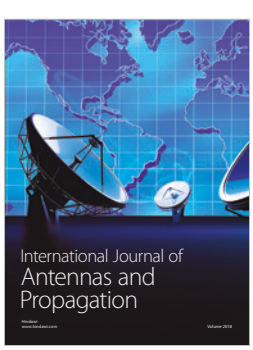

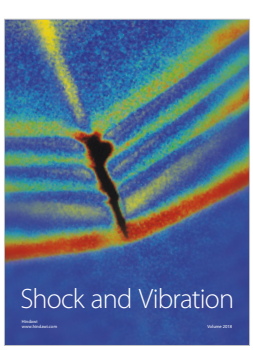

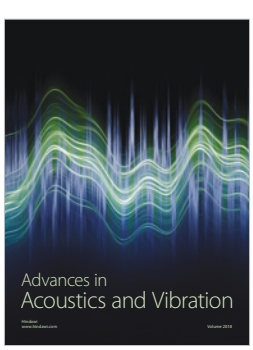

Hindawi

Submit your manuscripts at
www.hindawi.com